

Wind turbine lifetime extension decision-making based on structural health monitoring

T. Rubert^{a,*}, G. Zorzi^a, G. Fusiek^b, P. Niewczas^b, D. McMillan^a,
J. McAlorum^b, M. Perry^c

^a*Doctoral Training Centre in Wind and Marine Energy Systems, University of Strathclyde, 204 George Street, G1 1XW, Glasgow, UK*

^b*Department of Electronic & Electrical Engineering, University of Strathclyde, 204 George Street, G1 1XW, Glasgow, UK*

^c*Department of Civil & Environmental Engineering, University of Strathclyde, Glasgow G1 1XJ, UK*

Abstract

In this work, structural health monitoring data is applied to underpin a long-term wind farm lifetime extension strategy. Based on the outcome of the technical analysis, the case for an extended lifetime of 15 years is argued. Having established the lifetime extension strategy, the single wind turbine investigated within a wind farm is subjected to a bespoke economic lifetime extension case study. In this case study, the local wind resource is taken into consideration, paired with central, optimistic, and pessimistic operational cost assumptions. Besides a deterministic approach, a stochastic analysis is carried out based on Monte Carlo simulations of selected scenarios. Findings reveal the economic potential to operate profitably in a subsidy-free environment with a P90 levelised cost of energy of £25.02 if no component replacement is required within the nacelle and £42.53 for a complete replacement of blades, generator, and gearbox.

Keywords: structural health monitoring; wind turbine; lifetime extension; fatigue analysis; remaining useful lifetime; levelised cost of energy

*Corresponding author

Email address: tim.rubert@strath.ac.uk (T. Rubert)

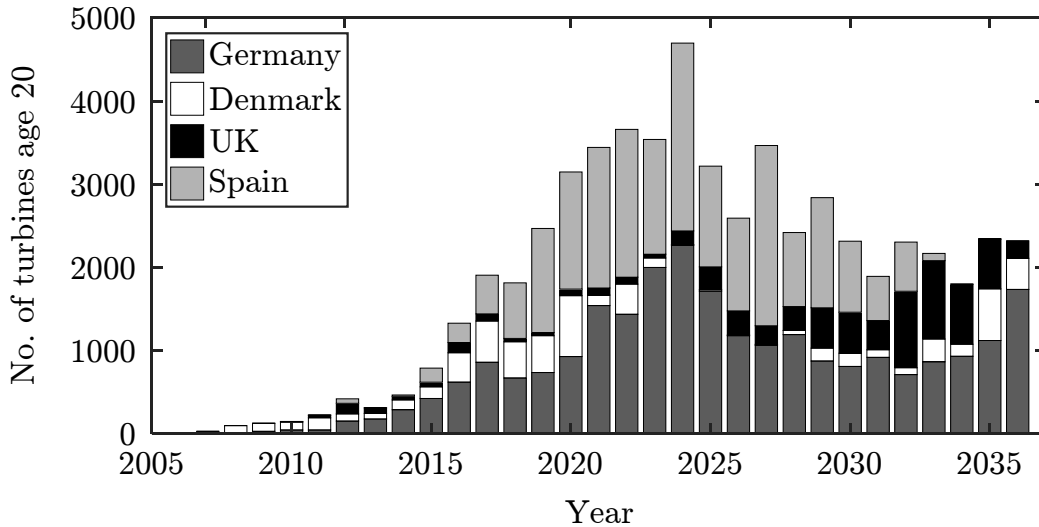


Figure 1: Turbines reaching end of design life by year [1].

1. Introduction

As highlighted by Ziegler et al. [1] in Figure 1, an increasing number of wind turbine generators (WTG) are reaching their end of design life. For this growing share of WTGs, a justification for lifetime extension may be based on different operational metrics such as: (i) the site classification, for example a turbine designed for a class II site but operated in a class III, (ii) the level of downtime, (iii) the lifetime energy production, (iv) sufficient design reserves, (v) if components are replaced during the design lifetime, and (vi) any combination of the above.

The main advantages of lifetime extension are: (i) the ability to increase the return on investment, with significantly less resources than required in repowering scenarios, (ii) utilise assets until the end of life cycle, thus preventing premature dismantling as well as (iii) using readily available local infrastructure (grid connection, access routes, community ties).

It has been proposed that structural health monitoring (SHM) may play an important role in supporting the process of lifetime extension (LTE) decision-making in order to reduce uncertainty of a turbine's site specific loading or if components are considered critical based on inspections [1, 2, 3].

Therefore, this paper applies SHM data from an operational wind turbine to develop an LTE strategy. Subsequently, the proposed strategy is con-

21 sidered jointly with operational data and subjected to an economic decision-
22 making methodology developed by Rubert et al. [4, 5]. In order to consider
23 uncertainties in the bespoke wind turbine economic model, uncertainty bands
24 are applied in cost and mean annual energy production. In addition a Monte
25 Carlo simulation is executed for selected scenarios.

26 The remainder of this paper is structured as follows. Section 2 compares
27 SHM activities with other forms of analysis to support the lifetime exten-
28 sion decision-making, presents a review of wind turbine tower and founda-
29 tion SHM research, and the results from the SHM measurement campaign.
30 Section 3 presents the applied LTE decision-making methodology whilst In
31 Section 4, the case study is presented where a strategy is derived and eco-
32 nomic input parameters presented. Results of the case study are presented in
33 Section 5, followed by a discussion of the key findings in Section 6. Finally,
34 conclusions outlining the key findings are presented in Section 7.

35 **2. SHM for Lifetime Extension**

36 Lifetime extension decision-making can be based on (i) data analysis,
37 (ii) inspections, (iii) aero-elastic simulations, and (iv) gathered data through
38 SHM systems. Inspections generate an in-depth assessment of structure’s
39 early failure indicators. However, inspections are only valid for a certain
40 period. As such, frequent assessment is necessary in either 6 or 12 months
41 intervals, thus lacking the ability to support the long-term business case
42 evaluation. Data analysis using SCADA is observed with caution, as the
43 information is often lacking temporally detailed operational history. Aero-
44 elastic simulations may generate a detailed analysis; however, simulations
45 require operational data that might have significant uncertainties, if e.g.,
46 taken from SCADA data. Additionally, aero-elastic simulations are generally
47 costly to carry out.

48 SHM concepts have the ability to provide long-term and in-depth data
49 that can be applied to generate the long-term business case, while delivering
50 a reduced uncertainty in the evaluation.

51 *2.1. Literature Review of SHM Concepts for Wind Turbine Towers and Founda-* 52 *tions*

53 With regards to tower sensor installation and data assessment practices,
54 the reader is referred to Smarsly et al. [6] for a 500 kW wind turbine, Rebelo
55 et al. [7, 8] for a 2.1 MW wind turbine, Loraux and Brühwiler [9] for a 2

56 MW wind turbine, and Botz et al. [10] for a 3 MW hybrid turbine consisting
57 of a concrete and steel tower section. The 2 MW wind turbine tower fatigue
58 analysis results in a remaining useful lifetime (RUL) of 135 years in a low
59 mean wind speed region (5.9 m/s) [9].

60 Related SHM concepts of onshore wind turbine foundations are available
61 by Currie et al. [11, 12] aimed at monitoring the displacement between the
62 tower and foundation. Based upon this work, Bai et al. [13] evaluate sensors
63 embedded in concrete blocks, to monitor the displacement and crack devel-
64 opment at the bottom of the inserted can flange that area is prone to failure
65 initiation. In this project, empty steel tubes are further vertically inserted
66 in the foundation, facilitating horizontal ultrasonic testing, to identify the
67 structural integrity with height. In addition, Perry et al. [14] and McAlorum
68 et al. [15] present a short and long term crack monitoring solution of wind
69 turbine foundations, whereas Rubert et al. [16] demonstrate a field case
70 study of embedding optical strain gauges in reinforced concrete foundations.

71 The interested reader is referred to [17, 18, 19] for a general review of
72 SHM opportunities, failures, and inspection practices of wind turbines.

73 *2.2. SHM Campaign*

74 The WTG of focus is a multi-MW, individual pitch regulated, onshore
75 generator located in Scotland. Due to confidentiality reasons, the type, man-
76 ufacturer, and rated power are not disclosed. In addition, all presented data
77 is normalized or the axis labels and tics are removed. The overall SHM
78 installation process, characterisation, temperature compensation, and valid-
79 ation is detailed in Ref. [20]. In comparison to other tower RUL assessments,
80 in this work, a turbine with a greater mean wind speed (> 7 m/s) and greater
81 rated power (> 3 MW) undergoes a load measurement campaign using op-
82 tical strain gauges at the tower base sampled at a high frequency (> 50 Hz).
83 The overall procedure of the fatigue analysis is taken from available and
84 previously mentioned publications; however, the novelty is to apply SHM in-
85 formation to derive and evaluate the long-term strategic LTE business case
86 for a specific wind farm.

87 *2.2.1. Tower SHM*

88 Ideally, strain gauges are installed at the locations on the tower situated
89 in the prevailing wind direction. However, the installation of tower sensors
90 might not be feasible in all areas; access restrictions and risk of damage due
91 to maintenance processes can limit the available positioning of sensors (e.g.

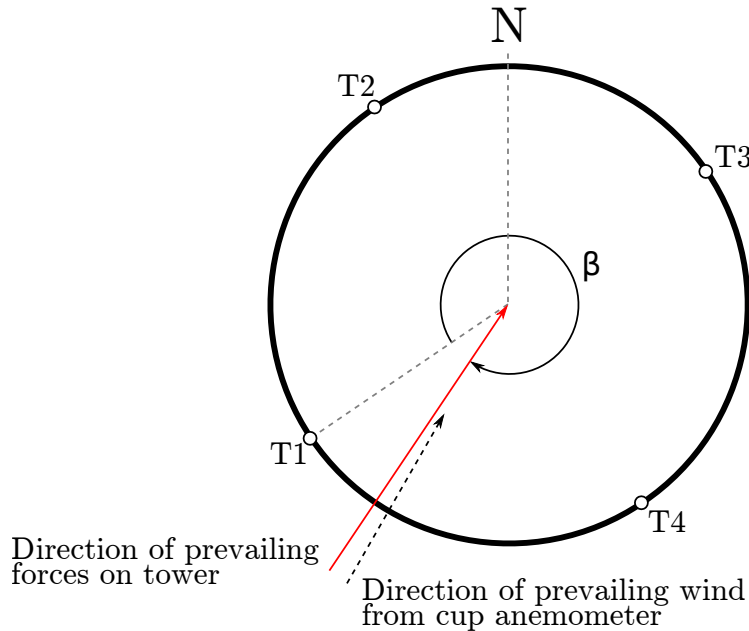


Figure 2: Schematic of tower sensor positions with respect to prevailing wind direction.

92 in proximity to the foundation-tower bolts that require servicing). Such con-
 93 straints were encountered in this work; however, as explored below, the prob-
 94 lem of imperfect positioning of sensors has not been of serious consequence
 95 to the adopted methodology.

96 The locations of the tower base strain gauges (T1–T4) with respect to
 97 north is illustrated in Figure 2. The normalised strain data, paired with
 98 30 minute average supervisory control and data acquisition (SCADA) wind
 99 speed data (in the respective directional corridor $\pm 10^\circ$) is illustrated in
 100 Figure 3 for T1 and in Figure 4 for the 90° rotated tower strain T2, re-
 101 spectively. Overall, the measurements are well in agreement with the yaw
 102 reference SCADA data, allowing confidence in the nacelle sensor calibration.

103 Based on the measurement campaign, as expected due to access con-
 104 straints, the sensors are not aligned with the prevailing wind direction. This
 105 was confirmed (i) based on the mean SCADA nacelle direction and (ii) since
 106 the operational SCADA period of T1’s inflow corridor ($\pm 10^\circ$) over the total
 107 recorded time covered 7.5% and 3.2% for T2, respectively.

108 In order to evaluate a component’s total lifetime based on measured or

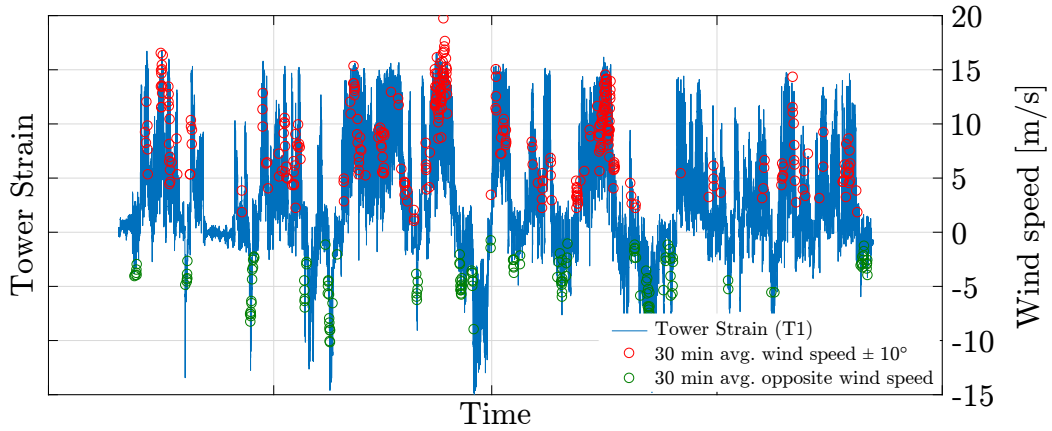


Figure 3: Strain data of base tower measurement (T1). The data is paired with recorded SCADA wind speed measurements on the right y-axis.

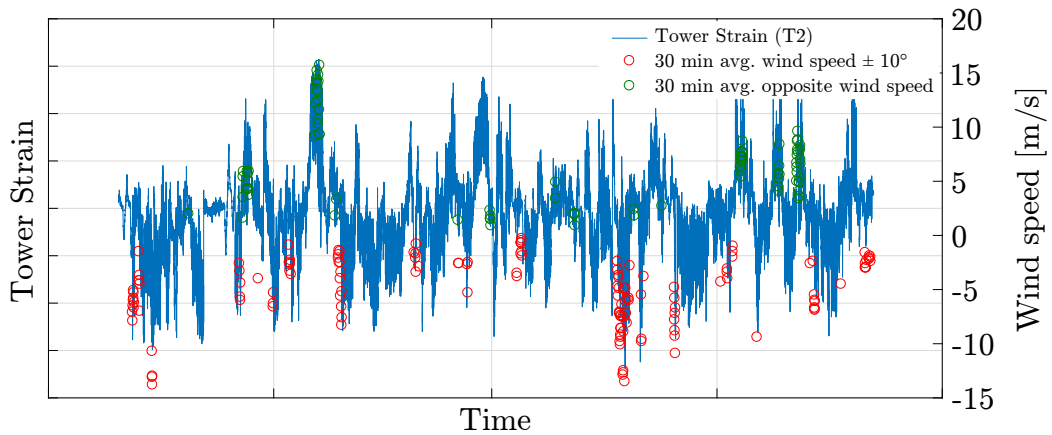


Figure 4: Strain data of 90° rotated base tower measurement (T2). The data is paired with recorded SCADA wind speed measurements on the right y-axis.

109 simulated data, the recorded signal is decomposed in defined discrete cycle
 110 ranges and each range's total number of occurrence is counted through a
 111 process referred to as rainflow counting [21]. Since, the rainflow counting
 112 algorithm is highly sensitive to changes in the maximum strain as well as
 113 in the frequency of occurrence of each range [9], the actual prevailing wind
 114 direction requires evaluation.

Given that the tower is radially symmetrical and the component's material (S355 steel) is designed to operate in its elastic limit, the stress across the circumference of the tower can be found as a vector sum of the stresses from the sensors. The two sensor strain measurements $v_{T1}(t)$ and $v_{T2}(t)$ respectively from T1 and T2, being positioned on the tower at 90° from each other allows calculation of the magnitude of the resulting vector, $|v(t)|$, and angle, $\gamma(t)$, by:

$$|v(t)| = \sqrt{v_{T1}(t)^2 + v_{T2}(t)^2} \quad (1)$$

$$\gamma(t) = \tan^{-1} \left(\frac{v_{T1}(t)}{v_{T2}(t)} \right). \quad (2)$$

115 The direction of the prevailing forces on the tower (which in turn is dic-
 116 tated by the prevailing wind direction), is identified counting the number
 117 of occurrences in the angle $\gamma(t)$ using a moving window of 5° as illustrated
 118 in Figure 5. The prevailing wind direction β with respect to T1 is then
 119 identified as the angle with the maximum number of occurrences.

120 Figure 5 indicates that the actual prevailing wind direction does not coin-
 121 cide with any sensor positions as it is not a multiple of 90° . In fact, the actual
 122 prevailing wind direction is shifted by 22° counterclockwise with respect to
 123 T1, which is also closely in agreement with the nacelle's mean SCADA dir-
 124 ection with a difference of 3° as illustrated in Figure 2.

Further, it is necessary to determine if the strain is positive or negative for the rainflow counting as the range (tension and compression) dictates fatigue cycles. Therefore, the difference between angles is calculated:

$$\alpha(t) = \beta - \gamma(t) \quad (3)$$

and the strain variation over time in the prevailing wind direction, denoted as $A(t)$ is calculated by:

$$A(t) = \cos(\alpha(t)) \cdot |v(t)|. \quad (4)$$

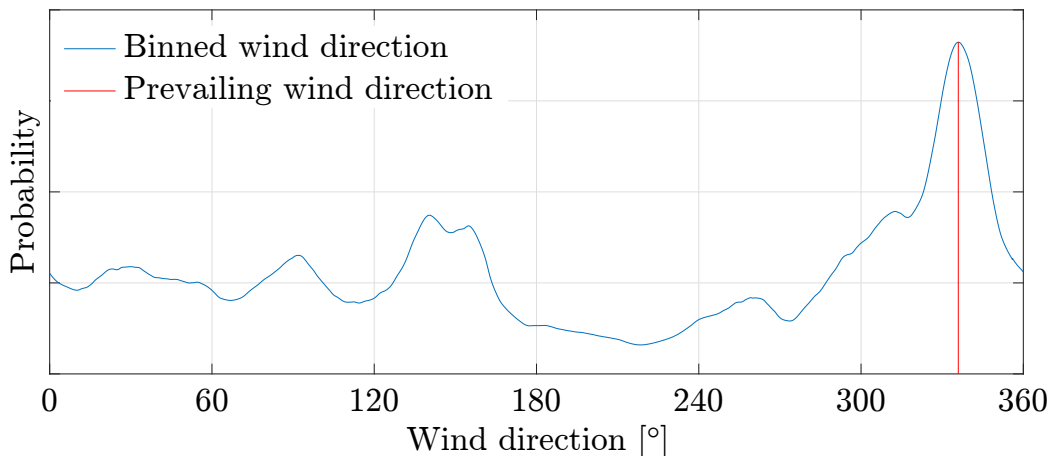


Figure 5: Identification of prevailing wind direction, β based on $\gamma(t)$ binning. The data is derived from tower strain sensor T1 & T2.

And for the perpendicular direction as:

$$B(t) = \sin(\alpha(t)) \cdot |v(t)|. \quad (5)$$

125 It was further verified that of this new set of axes, the higher frequented
 126 component is selected.

127 Figure 6 displays the calculated strain in the prevailing wind direction.
 128 The strain profile is in agreement with the wind speed measurements from the
 129 SCADA data. Also, the SCADA data shows that, in the operational corridor
 130 considered, the turbine was operational for 23% of the total recorded time.
 131 This corroborates the above analysis.

The tower is usually made from hot-rolled steel, welded together circumferentially and longitudinally [22], with welded flanges at either tower end. As such the S-N curve assumption is dependent on the weld type [23]. The rainflow counting algorithm was applied according to the ASTM standard where half cycles are conservatively treated as full cycles [21, 24]. The S-N curve for the tower is used with the following parameters. The endurance limit at 2 million cycles, $\Delta\sigma_C = 80$ MPa [25, 23], the constant amplitude fatigue limit at 5 million cycles, $\Delta\sigma_D = 59$ MPa, and the cut-off limit, $\Delta\sigma_L = 32$ MPa according to EN 1993-1-9 [23]. With the established S-N curve, Miner's damage calculation was applied, after the strain was transformed into a stress (Young's Modulus, $E = 200$ GPa). The cumulative

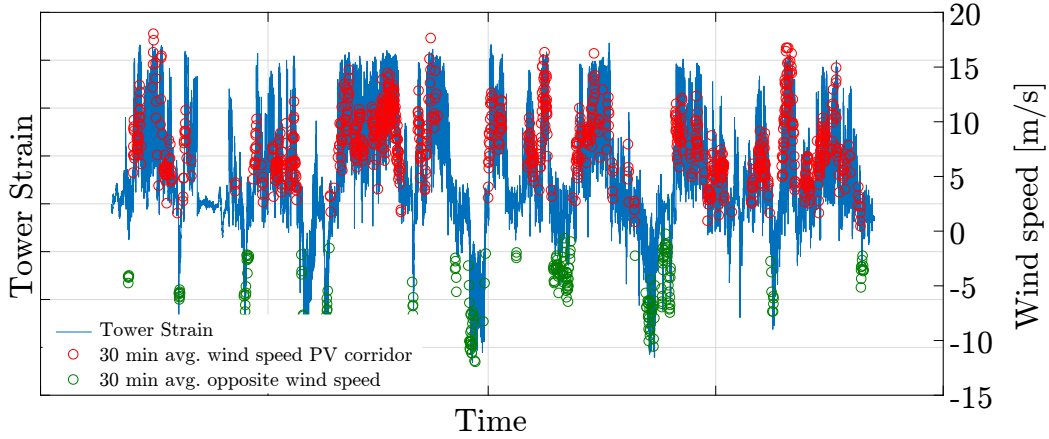


Figure 6: Strain data of derived prevailing wind direction. The data is paired with recorded SCADA wind speed measurements on the right y-axis.

fatigue damage D_{tot} is:

$$D_{tot} = \sum D_i \quad (6)$$

where D_i is the partial damage in each discretised rainflow counting bin i . D_i is thus:

$$D_i = S_m^{-m} \sum_i^N n_i \sigma_i^m \quad (7)$$

132 where S_m as well as m are material constants, and σ the stress amplitude with
 133 n numbers of observed occurrences for the respective bin i . If $\Delta\sigma_i > \Delta\sigma_D$,
 134 $m = 3$ and if $\Delta\sigma_L < \Delta\sigma_i < \Delta\sigma_D$, $m = 5$. Otherwise, $D_i = 0$. The total
 135 fatigue damage D_{tot} is thus calculated. The binning width of the rainflow
 136 counting algorithm and sampling frequency determine the accuracy of the
 137 lifetime prediction; however, a high sampling frequency in combination with
 138 a small binning width, significantly increase processing requirements. As
 139 such, the appropriate binning width of 0.2 MPa was identified as illustrated
 140 in Figure 7 while an appropriate minimum sampling frequency is identified
 141 as 100 times the first tower mode as illustrated in Figure 8.

142 The total tower lifetime, based on the recorded measurement data $T1$
 143 was thus estimated to be 248 years and for $T2$ 339 years, respectively. In the
 144 prevailing wind direction, the derived and more frequented corridor β , the
 145 lifetime analysis resulted in a reduced lifetime of roughly 23 years with a total

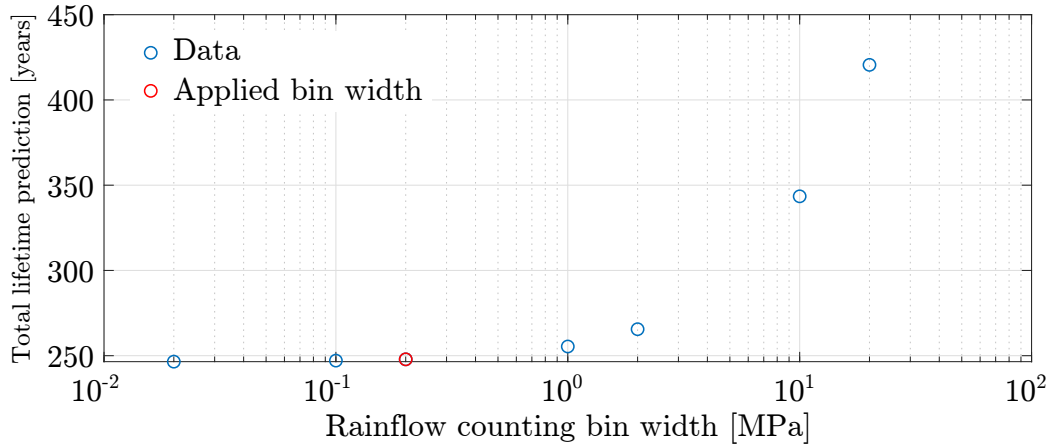


Figure 7: Impact of binning width on lifetime prediction. Applied frequency is 380 times the first tower mode.

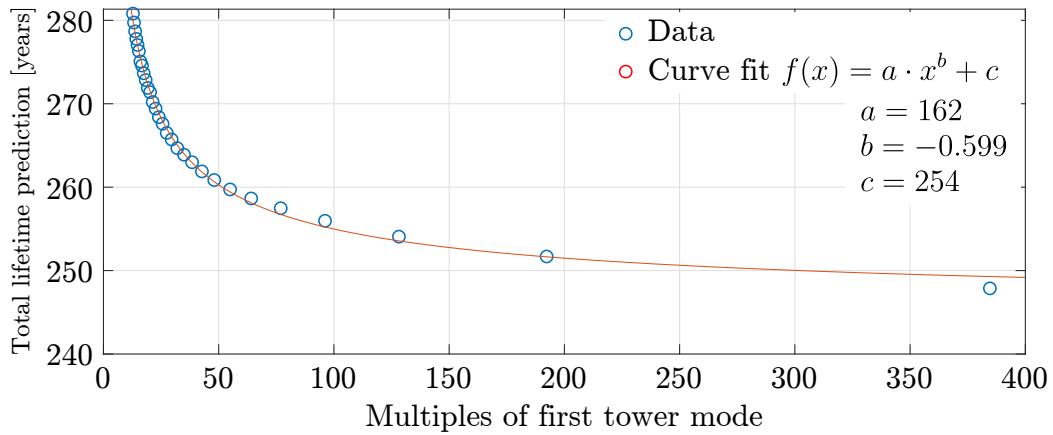


Figure 8: Impact of sampling frequency on lifetime prediction based on a 0.2 MPa binning width.

146 of 225 years¹. The magnitude of this reduction further allowed confidence in
147 the data processing. In order to verify this result, the lifetime analysis was
148 carried out for varying β (0-180°) as more significant loading, albeit with an
149 overall lower number of occurrence, could have been experienced for wind
150 directions off the prevailing axis. This analysis verified the prevailing wind
151 direction β , identified in Figure 5.

152 Further, based on findings by Rebelo et al. [7, 8] and Loraux and Brühwiler
153 [26], the maximum tower stress is likely to be experienced at 30-40% of the
154 hub height. At present, the complete tower geometry of the considered wind
155 turbine is unknown. Therefore, a conservatively selected correction factor,
156 derived from the previously mentioned tower monitoring campaigns, is in-
157 troduced. The corrected total lifetime at the critical tower height is thus
158 identified as 81.6 years. A further correction is required as the outer shell of
159 the tower has a greater stress, as the inner walls' strains are monitored. Thus
160 this correction leads to a total lifetime of 78.4 years. So far, the carried out
161 stress correction procedure has neglected any reliability aspects. In order to
162 allow for sufficient safety margins, the IEC power production safety factor
163 (1.25) is further applied. With the safety factor included, the total lifetime
164 results in 34.6 years. The overall data processing steps are further illustrated
165 in Table 1. If residual cycles of the rainflow counting process are treated as
166 half cycles, as suggested by the IEC 61400-13 standard [27], the total lifetime
167 is identified as 35.2 years.

168 Overall, from the point of view of the tower, a LTE of 15 years thus
169 appears feasible, given considerate safety margin, as the carried out fatigue
170 analysis reveals a total lifetime of 35 years (turbine design life is 20 years).

171 2.2.2. Foundation SHM

172 Overall, SHM of wind turbine foundations is a challenging area of re-
173 search as highlighted by several studies, since the foundation is mainly in-
174 accessible for inspection [13, 14, 20]. Given that wind turbine foundations
175 (i) are designed for a lifetime of 50 years or more, (ii) their design is based
176 on conservative assumptions, and (iii) they are structurally of key import-
177 ance, there is little concern to accommodate for LTE. Based on an internal
178 strain analysis of the reinforcement cage by Rubert et al. [20], this is further
179 supported. As a consequence, from an economic lifetime extension decision-

¹binning width of 0.2 MPa and frequency of 380 times the first tower mode

Table 1: Process of Data Manipulation. PW: prevailing wind, HC: height correction, SC: section correction, SF: safety margin. Frequency of 380 times the first tower mode.

Analysis	RUL [years]	Comment
T1 (tower base)	248	Sensor 22° to prevailing wind
T2 (tower base)	339	Sensor 112° to prevailing wind
PW (tower base)	225	Derived prevailing wind with Equation 4
PW + HC	81.6	Corrected stress at most critical height
PW + HC + SC	78.4	Corrected for the outer shell
PW + HC + SC + SF	34.6	Added IEC safety margin

180 making perspective, the foundation is not of concern (except when severe
181 cracks are encountered). “Cracking is normal in reinforced concrete struc-
182 tures subject to bending, shear, torsion or tension resulting from either direct
183 loading or restraint or imposed deformations” [28]. Although cracking is ex-
184 pected to some degree, there is a crack width limit, w_{max} that is governed
185 under the service limit state. The acceptable crack width is dependent on
186 the concrete exposure class and type of reinforcement and can be looked up
187 in design codes and guidelines. Also, if cracks appear, work by Perry et al.
188 [14] and McAlorum et al. [15] may be applied for SHM. Results thus reveal
189 a possibility of an extended WTG operation of greater than 15 years.

190 3. Lifetime Extension Methodology

The lifetime extension decision-making methodology is schematically il-
illustrated in Figure 9, where the lifetime extension period is treated as a sep-
arate investment and calculated based upon levelised cost of energy (LCOE₂).
To calculate LCOE₂, the net present value (NPV) of costs is divided by the
NPV of the annual energy production (AEP):

$$LCOE_2 = \frac{NPV_{costs}}{NPE} = \frac{C_0 + L_0 + \sum_{n=1}^T \frac{F_n + O_n + V_n}{(1+d)^n}}{\sum_{n=1}^T \frac{E_n}{(1+d)^n}} \quad (8)$$

191 where NPE is the net present energy, C_0 the equity capital expenditure of
192 component replacements (CAPEX_{Replace,E}), L_0 the lifetime extension capital
193 expenditure (CAPEX_{LTE}), n is the period ranging from year 1 after the
194 design lifetime to T the final year of operation (end of extended lifetime), F_n

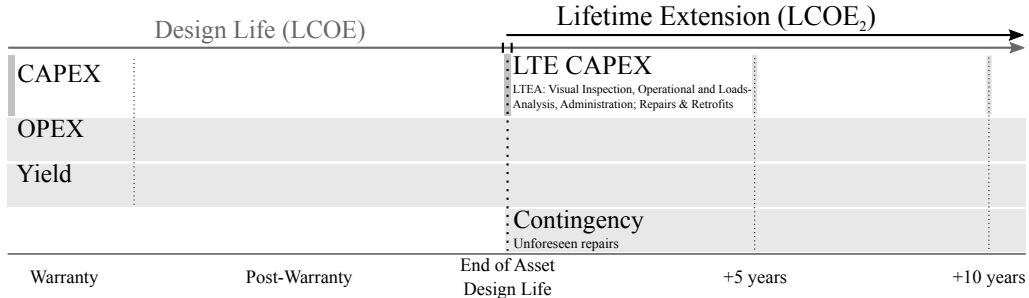


Figure 9: Lifetime extension decision methodology [4].

195 the constant annuity payment of the component replacement’s expenditure
 196 debt in period n ($CAPEX_{\text{Replace},D}$), O_n the fixed operating cost including
 197 decommissioning² in period n , V_n the variable operating cost in period n , E_n
 198 the energy generated in period n , and d the discount rate.

199 This extended lifetime methodology is equipped with operational data in
 200 terms of cost and yield parameters. The prior includes the CAPEX LTE
 201 and operational & maintenance (O&M) expenditure and the latter identified
 202 through operational knowledge or alternatively the application of a Weibull
 203 wind distribution in combination with a turbine’s power curve [29]. Of course
 204 all variables are ideally based upon the operational design lifetime and may
 205 be adjusted depending on; e.g., failure and reliability data.

206 4. Lifetime Extension Case Study

207 4.1. Strategy

208 The structural integrity of the foundation and tower is one of the main
 209 factors in determining economic lifetime extendibility (high replacement costs)
 210 and the high importance in serving as a load-carrying component, their RUL
 211 is of significant interest for a given wind turbine. As previously discussed, the
 212 foundation design lifetime significantly exceeds other components, provided
 213 that the design and construction procedures have been correct. Hence, in

²onshore it is expected that the scrap value equalises decommissioning costs; offshore this is certainly not the case

214 the great majority of cases, the tower RUL is of greater concern. There-
215 fore, knowledge of the site-specific tower RUL will provide argument for the
216 long-term economic business case.

217 The results from the SHM campaign presented above indicate that life-
218 time extension of 15 years appears feasible. Therefore, for the LTE business
219 case the strategic extension period is considered to be 15 years.

220 4.2. Input Data

221 The input data for the economic model is a combination of actual and
222 generic data as illustrated in Table 2. Where possible, real input is applied;
223 however, the commercial business case is highly sensitive, thus not all actual
224 data is applied in the model. As such, the economic model generates an
225 academic case scenario that is aligned as best as possible to a potential real
226 scenario. The power curve was reproduced as highlighted by Rubert et al.
227 [4]; however, rather than applying the maximum power coefficient, $C_{p,\max}$ to
228 derive the power curve, C_p varies with wind speed, $C_p(v)$ that was derived
229 based on the manufacturer’s data sheet ($\rho = 1.225 \text{ Kg/m}^3$). This enables
230 greater accuracy in the yield modeling as outlined by Carillo et al. [30] and
231 Lydia et al. [31]. As identified by [4, 32], the mean wind speed has the highest
232 magnitude in the impact, thus careful evaluation is necessary. The turbine’s
233 mean wind speed was derived using operational SCADA data, accounting
234 for the impact of curtailment (provided by the operator). Curtailment was
235 included in the model by reducing the average wind speed for the specific
236 wind turbine.

237 Given that the foundation and tower are able to facilitate the target
238 lifetime extension period, components along the drive train may require re-
239 placement. This is budgeted as CAPEX_{SPARE,D} and CAPEX_{SPARE,E} with a
240 70/30% debt-equity split, the latter budgeted as a constant annuity with the
241 interest rate set as 3.5% [33]. Cost and time assumptions for the necessary
242 crane (1,200 t) and service team for component replacements were evaluated.
243 The time requirement was increased by 50% and the service team number
244 increased by 25% from those from [4]. The overall cost assumptions are sum-
245 marised in Table 3 for the central case as well as optimistic and pessimistic
246 scenario, respectively.

247 The discount factor is assumed at 7.5%, with inflation set at 1.5% ac-

Table 2: Wind turbine parameters. Actual are real operational parameters for the respective wind turbine, while generic data is applied due to confidentiality in the business case. The resulting capacity factor is a combination as actual and generic data is applied to derive the metric.

Parameter	Value	Actual/Generic Data
Cut-in wind speed	3 [m/s]	Actual
Cut-out wind speed	25 [m/s]	Actual
Rated wind speed	12.5 [m/s]	Actual
Rotor diameter	Not disclosed	Actual
Wind speed	Not disclosed	Actual
Power coefficient	Not disclosed	Actual
Turbulence intensity	0.1	Generic
Availability	97 [%]	Generic
Wake & park losses	10 [%]	Generic
Discount factor	7.5 [%]	Generic
Inflation	1.5 [%]	Generic
Weibull shape factor	2	Generic
Resulting capacity factor	Not disclosed	Actual/Generic

248 counted to administration and spare parts of the O&M expenditure³.

249 Also, for the scenario with no component replacement, an annual per-
 250 formance degradation of 0.3% is modeled based on findings by [35, 36, 5]. In
 251 the other scenarios, due to component upgrades the performance degradation
 252 is likely significantly smaller and thus neglected.

253 To get greater confidence limits, a Monte Carlo simulation is further
 254 applied based on the application of normal distributions. This allows to
 255 account for statistical factors, as component/installation costs and the wind
 256 inflow parameters may vary over time. As such, variability in the results
 257 are expected⁴. This was carried out for the scenario with no component
 258 replacement and the exchange of the entire drive train. The annual wind
 259 speed was characterised based on SCADA mean data paired with a standard
 260 deviation of 7% [39]. The cost data was modeled with a standard deviation
 261 of 25% as illustrated in Table 3. For the component replacement process, if

³The interested reader is referred to [34] for detailed commentary on LCOE input parameters.

⁴For detailed information of Monte Carlo simulations, the reader is referred to [37, 38].

Table 3: Generic lifetime extension cost estimations for a wind farm [4]. The range interval is applied in the Monte Carlo simulation, with the central parameter defined as the median value.

Parameter	Central	Range	Unit
O&M			
Fixed	30,192	22,644-37,740	£/MW/y
Variable	5.1	3.83-6.38	£/MWh
Insurance	2,226	1,669-2,782	£/MW/y
Connection charges	3,810	2,857-4,762	£/MW/y
CAPEX LTE			
Visual inspection	2,689	2,017-3,361	£/WTG
Loads analysis	3,500	2,625-4,375	£/WTG
Operations analysis	2,000	1,750-2,250	£/WTG
Administration	1,000	750-1,250	£/WTG
Spare parts			
3 blades	238,560	178,920-298,200	£/WTG
Gearbox	147,680	110,760-184,600	£/WTG
Generator	93,152	69,864-116,440	£/WTG
Installation expenditure			
Crane Mob/Dmob	20,000	15,000-25,000	£/Wind Farm
Crane operation	2,000	1,500-2,500	£/day
Service personal	58	43.1-71.9	£/h

262 the wind speed is above a certain wind speed threshold, components cannot
263 be lifted. Therefore, the required crane and service hours were applied based
264 on the minimum expected time and a normally distributed time component
265 added to account for wind related delays. Based on the procedure detailed
266 by Vose [37], the number of required iterations n was identified as 50,000
267 based on a standard error of 3% and a 90% confidence interval.

268 5. Results

269 When operating a wind farm, each turbine can be characterised differ-
270 ently; i.e., some turbines have greater average wind speeds than others, de-
271 pending on the local terrain, wake effects, and operational parameters. With
272 regards to LCOE calculations, the mean wind speed has the greatest im-
273 pact [32, 4]. When pairing the mean wind speed with operational know-
274 ledge (downtime, degradation, curtailment, etc.) the AEP or capacity factor
275 can be derived. Therefore, when operating a wind farm that is reaching its
276 end of design lifetime with fewer revenues or when directly exposed to the
277 spot-market electricity price, some turbines might be less profitable in their
278 continued operation than others. As a consequence, a LTE decision-making
279 requires turbine specific evaluation.

280 The lifetime extension $LCOE_2$ of the bespoke economic turbine model
281 based on operational wind conditions are illustrated in Figure 10 under the
282 assumption of (i) no retrofit and (ii) the exchange of the entire drive train;
283 in Figure 11 for a single retrofit of a drive train component; and in Figure 12
284 for any retrofit combination of drive train components. As mentioned before,
285 each scenario has an assumed extended lifetime of 15 years.

286 The error bands are based on the cost variation illustrated in Table 3.
287 A wind farm usually consists of several individual turbines, with varying
288 degree of loading and electricity production, thus when it comes to lifetime
289 extension, not necessary all turbines are economically suitable to keep in
290 operation. Knowing that the annual wind speed and hence AEP has the
291 greatest impact on LCOE, the wind speed is varied in order to determine
292 profitability of the different cases.

293 With turbines mostly being exposed to the subsidy-free spot market elec-
294 tricity price, a threshold is defined to determine individual turbine suitability.
295 This is defined as 10% below the average UK's spot market price of the past
296 5 years [4].

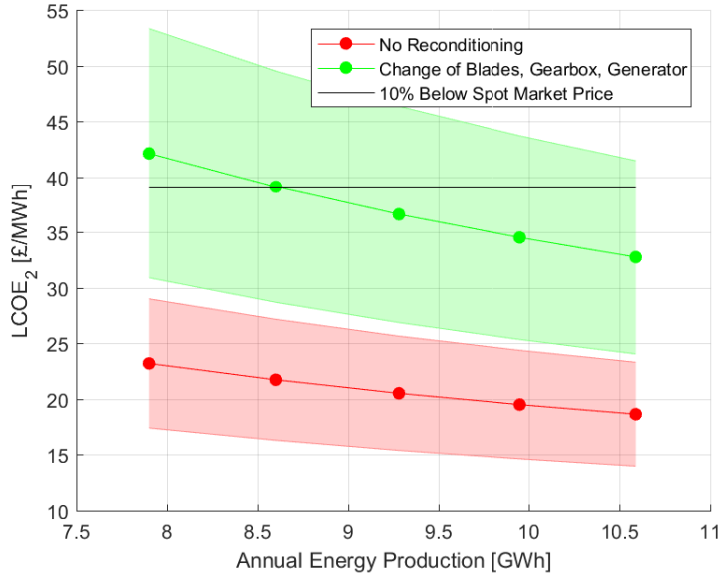


Figure 10: LCOE₂ of lifetime extension period with annual energy production (no retrofitting and drive train exchange).

297 Overall, without any component replacement, the LCOE₂ is significantly
 298 below the defined subsidy-free threshold (£39), hence LTE is supported for
 299 any of the modeled AEP cases. Alternatively, if the entire drive train requires
 300 replacement (blades, gearbox, and generator), this would only be economi-
 301 cally viable if the annual energy production is above 8.6 GWh/WTG. The
 302 complete range is illustrated in Figure 10.

303 For any single component exchange (blades, gearbox, and generator),
 304 all medium cost estimates are below the threshold; however, for the pess-
 305 imistic cost scenario, the replacement of blades are economically infeasible
 306 and decommissioning is advised as illustrated in Figure 11 when below 8.3
 307 GWh/WTG.

308 For any two component replacement scenario, the cases including new
 309 blades require at least 7.5 GWh/WTG when paired with a generator ex-
 310 change, and 7.8 GWh/WTG when paired with a gearbox exchange in order
 311 to be economically viable as illustrated in Figure 12. The replacement of
 312 a gearbox in combination with the generator is feasible in the medium cost
 313 scenario; however, in a pessimistic scenario caution is required.

314 Table 4 further displays the annual available contingency with respect to

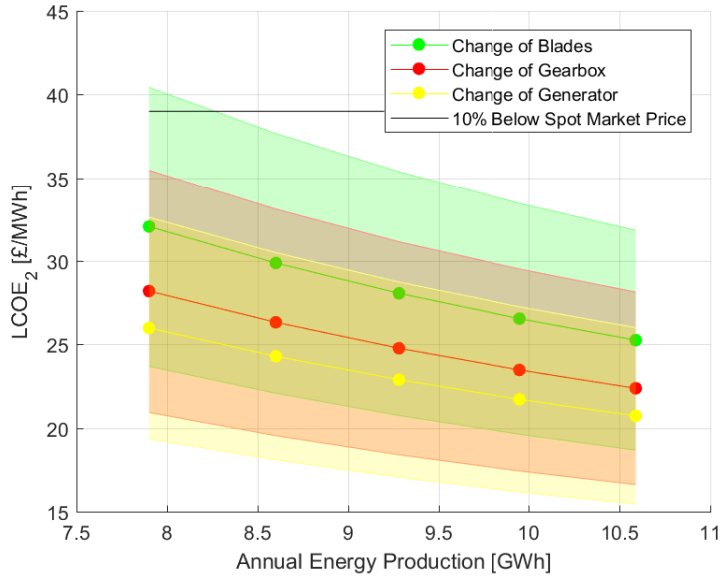


Figure 11: LCOE₂ of lifetime extension period with annual energy production (single retrofit).

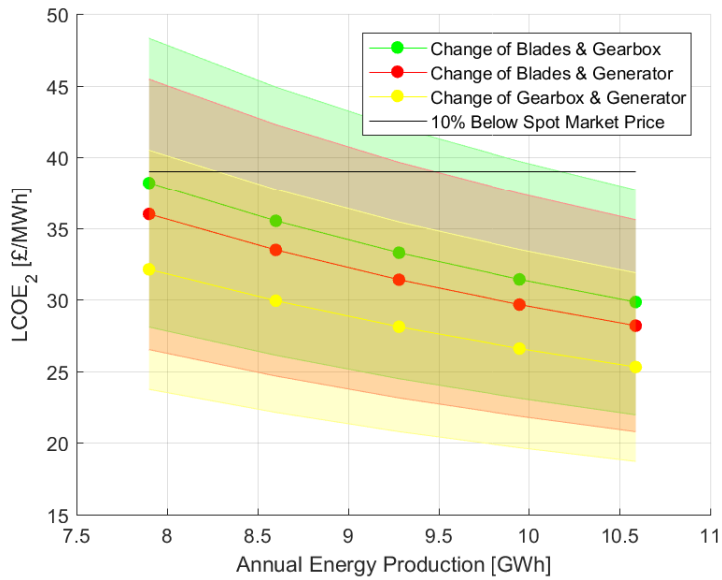


Figure 12: LCOE₂ of lifetime extension period with annual energy production (double retrofit).

Table 4: Annual Contingency [£] for 15 year LTE under different scenarios. N/A: costs exceed revenue.

Scenario	Pessimistic	Central	Optimistic
No reconditioning	141,363	186,268	231,173
Reconditioning of blades	37,704	104,901	173,560
Reconditioning of gearbox	76,837	135,610	195,286
Reconditioning generator	99,283	153,214	207,719
Reconditioning blades, gearbox, & generator	N/A	24,980	116,871
Reconditioning blades & gearbox	N/A	56,138	138,952
Reconditioning blades & generator	N/A	73,743	151,385
Reconditioning gearbox & generator	37,221	104,452	173,158

315 (i) the different replacement scenarios and (ii) the expenditure range based on
 316 an AEP of 9.3 GWh. As illustrated in Figure 9, this parameter indicates the
 317 potential money to spend before the project becomes non-profitable along the
 318 life extended period; i.e., when decommissioning is advised. The remaining
 319 contingency may be applied to support the operational LTE decision-making
 320 as the available budget indicates the risk of an aimed strategic decision.
 321 An example would be if the replacement of the drive train is strategically
 322 considered matched with central cost estimates, as the remaining annual
 323 contingency is £24,980/WTG. In such an event, if severe issues occur (such
 324 as a major generator or bearing failure), the project is likely more risky to be
 325 profitable than other decisions with a greater annual contingency. This risk
 326 can potentially be reduced by in-depth structural analysis and the application
 327 of reliability models based on inspection results.

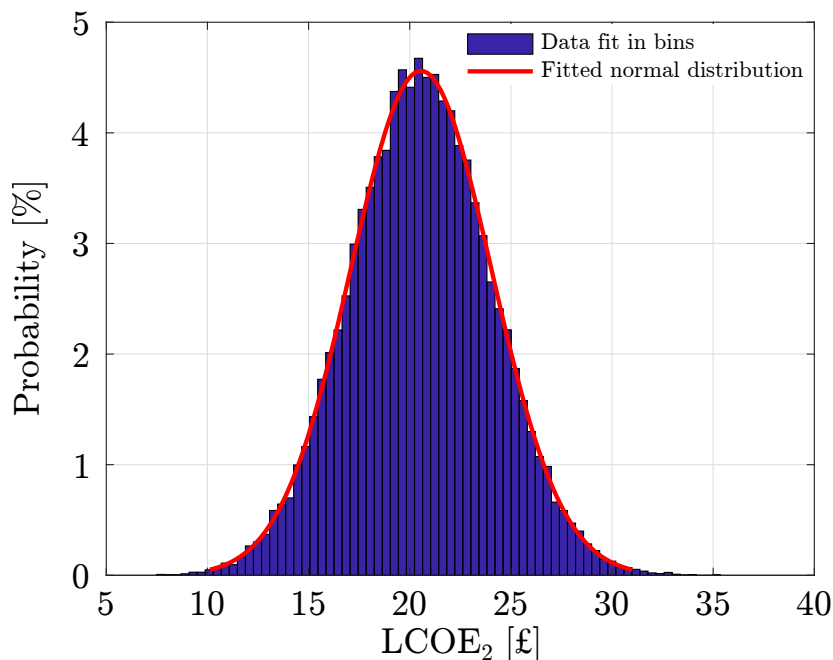


Figure 13: Monte Carlo analysis of LCOE₂ of no component replacement.

328 Results of the Monte Carlo simulation are presented in Figure 13 with no
 329 component replacement and in Figure 14 for the replacement of the entire
 330 drive train. In addition, Table 5 presents the respective P10/50/90 percent-
 331 iles.

Table 5: Project expenditure percentiles [£] based on Monte Carlo simulation.

Scenario	P10	P50	P90
No replacement	16.10	20.54	25.02
New drive train	31.68	37.07	42.53

332 Overall, there is a 90% probability that the LCOE₂ is below £25.02 with
 333 no component replacement, whereas when exchanging the entire drive train,
 334 there is a 50% chance that LCOE₂ are above £37.07. With respect to the
 335 threshold spot market electricity price, there is a 69% chance to be econom-
 336 ically profitable. Of course, results of the Monte Carlo simulation will change
 337 with differently encountered mean AEP.

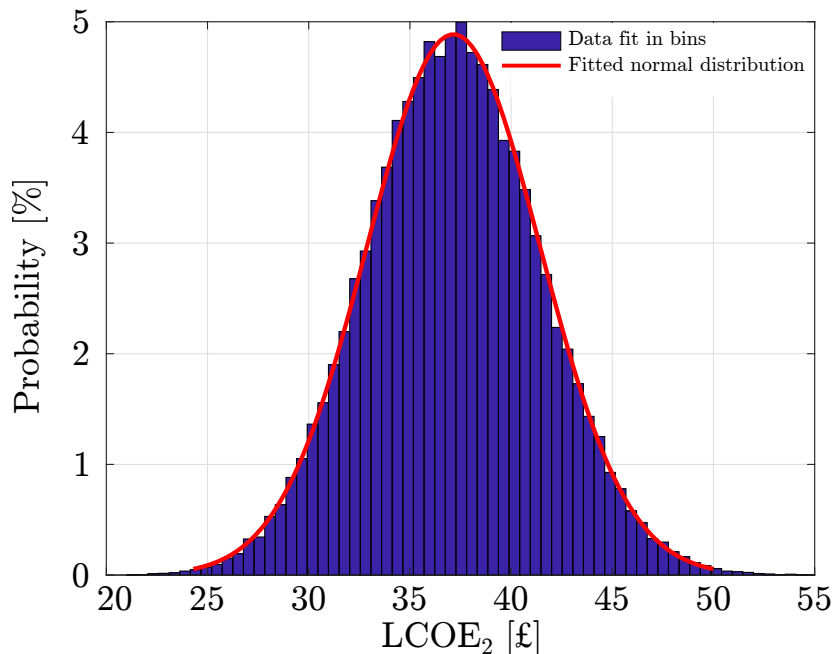


Figure 14: Monte Carlo analysis of LCOE₂ of drive train exchange.

338 **6. Discussion and Future Work**

339 Confidence in the SHM measurement campaign increases as a function of
 340 the duration of the data monitoring campaign; a longer monitoring period
 341 will thus deliver an increase in confidence in the strategic LTE business case.

342 Applying the AEP of each turbine requires closer examination as often
 343 turbines are curtailed due to network restrictions. Therefore, besides looking
 344 at the AEP in isolation, curtailment information can deliver a more accur-
 345 ate picture. Also, when having operated a wind farm for 20 years, its grid
 346 integration is well understood and thus data readily available.

347 As identified by Tavner [40], Wilson [41], and Reder [42], wind turbine
 348 reliability is correlated with environmental conditions. Thus, a turbine's
 349 components have an individual and thus varying load profile. Of course,
 350 the design of the respective turbine should accommodate for such differences
 351 given the IEC classes (IEC 61400-1). The turbine in question was identified
 352 based on the highest annual wind speed of the respective wind farm. Nev-
 353 ertheless, such indicators as turbulence intensity are also important. The
 354 O&M costs may therefore fluctuate per turbine and should ideally be taken

355 into consideration in the economic evaluation. In order to accommodate
356 fluctuations, the optimistic and pessimistic cost bands are presented.

357 While local wind conditions may change over the years [43, 44], so in turn
358 would the AEP. Therefore, when extracting the AEP, a period of several years
359 should be considered. Ideally, the entire operational life.

360 It is further possible to extrapolate tower fatigue findings onto each indi-
361 vidual wind turbine in the wind farm by application of a tower finite element
362 model and, ideally, analysis of high frequency SCADA data (if available).
363 This will be considered in future work, in order to determine a wind farm
364 lifetime extension strategy, by clustering turbines into cells with different
365 loading. In this regard, low wind speed and turbulence intensity exposed
366 wind turbines might be selected for turbine removal and the spare parts
367 might be stored or straight away used to replace turbine components with
368 higher mean wind speed and turbulence intensity values.

369 Judging from the cost to carry out a tower measurement campaign (roughly
370 £20,000-30,000), we argue that to gain an accurate LTE strategy, the benefit
371 outweighs the costs of the installation of such a system. Of course, the latter
372 depends on the deployed turbine and wind farm size [5] as well as the SHM
373 system design.

374 We further suggest to install tower sensor sets (one sensor each side for
375 validation purposes [20]) 90° apart as well as to analyse each wind corridor
376 by varying β in order to cover any eventualities if e.g., the assumed pre-
377 vailing wind direction does not match the real prevailing wind corridor as
378 highlighted in Section 2.2. In addition, as the cross sectional moment of
379 inertia and bending moment change with tower height, so does the stress
380 distribution. Ideally, the tower wall thicknesses and sectional diameters are
381 measured to derive the maximum stress location. Nevertheless, in the absence
382 of tower geometry data, correction factors may be applied as highlighted in
383 Section 2.2. Overall, we strongly recommend to measure the tower's geo-
384 metry (thickness and diameter with hub height) to identify the most critical
385 stress location. At this location, the fatigue analysis shall be carried out.
386 As such, the application of generic or simplified tower geometries may lead
387 to severe uncertainties and inaccuracies of aero-elastic simulations and thus
388 caution is advised.

389 The SHM monitoring campaign may be tailored for a global analysis
390 aimed at evaluating stresses of critical tower areas, such as along the entrance

391 door⁵ as well as flanges as discussed by Schedat et al. [46].

392 With respect to the rainflow counting algorithm, we suggest to use a bin-
393 ning width equal or lower than 0.2 MPa paired with a minimum sampling
394 frequency of 100 times the first tower mode. This allows accurate meas-
395 urements while maintaining an appropriate accuracy (within 10%). Also,
396 a correction parameter can be applied based on the findings presented in
397 Figure 7 and 8 if data is available at a lower sampling frequency.

398 SHM data combined with economic findings do not suggest that long-
399 term lifetime extensions should be carried out blindly, thus the necessary
400 inspections are key in making sure that the continued operation is safe. For
401 the tower, critical sections are welded and bolted connections as well as areas
402 with corrosion [3, 45]. An inspection guideline published by DNV GL for the
403 tower and foundation is presented in Table 6 of the Appendix. In addition,
404 an inspection guideline is published by Megavind [45]. In critical cases, it is
405 further suggested to reduce the inspection interval or to install tailored SHM
406 hardware. For an example of tower flange cracking, the reader is referred to
407 work developed by Do et al. [47]. To access experimental mechanical and
408 fracture properties of welded S355 steel, work by Mehmanparast et al. [48] is
409 suggested. We also recommend monitoring the first natural frequency as well
410 as damping ratio of the tower as variations can indicate structural changes
411 with little resources spend, if sensors are installed.

412 As illustrated by Helm [49] based on data by the Department for Busi-
413 ness, Energy, Industry, and Strategy (BEIS), the electricity price is expected
414 to remain at current prices and then gradually increase from 2020, reaching
415 a high in 2024 before dropping off in the UK. In fact, this requires careful
416 observation and scrutiny in order to define the profitability threshold appro-
417 priately.

418 Uncertainties further origin from the weld assumption; data that is not nec-
419 cessarily shared by turbine manufacturers. Potentially, the weld class might
420 be analysed with ultrasonic wall thickness measurement devices to get con-
421 fidence in the selection of the appropriate weld classes.

422 Finally, in comparison to previous findings by Rubert et al. [4], this work
423 derives the strategic lifetime extension case for a significantly greater rated

⁵According to the publication from Megavind, the tower entrance door is not considered as a critical area: "As for tower fatigue, cracks in the door-tower connection may, with low probability, occur when the turbine reaches the design lifetime" [45].

424 turbine taking the actual structural integrity into consideration as well as
425 the actual wind speed. As such, the lifetime extension business case appears
426 in general more positive than the assessment of smaller scale generators.

427 **7. Conclusion**

428 This work explores a strategic case specific lifetime extension decision-
429 making process, based on information gathered through SHM. The process
430 indicates that if the tower and foundation are in a good condition (acceptable
431 level of corrosion, no cracks for the tower; foundation cracks within acceptable
432 limit), these key turbine components are generally well suited to facilitate
433 lifetime extension decision-making.

434 Based on the SHM of the wind turbine tower, the total lifetime was
435 identified as 35 years by evaluation of the prevailing wind direction at the
436 most critical tower location, including a load safety margin. In addition,
437 parameters are provided for the analysis to derive the tower's RUL.

438 Forwarding the structural information to the economic business case, res-
439 ults suggest a P90 LCOE₂ of £25 if no components require reconditioning,
440 paired with a lifetime extension of 15 years. If the blades, gearbox, and gen-
441 erator are exchanged in year 20, the P90 LCOE₂ is identified as £42.50. For
442 this case, the probability to be 10 % below the average spot market price is
443 69%, thus caution and due diligence is advised or alternatively a lower profit
444 margin shall be defined.

445 Overall, the results of this study further support the operational know-
446 ledge that lifetime extension is highly site specific; however, it is essential to
447 derive a suitable LTE strategy for the continued operation to generate the
448 economic business case. This is especially valid for multi-MW turbines with
449 substantial annual energy production. Besides allowing continued electricity
450 generation and maintaining local O&M jobs, lifetime extension reduces the
451 generation of waste, which is of general interest.

452 **8. Appendix**

Table 6: Tower & foundation inspection guideline [3]. D is damage, C is cracks, Co is corrosion, Sp is safety sign plates, Ps is prestress, Cf is connection/fitting, and F is function.

Tower Component	Inspection
Tower structure	D,Co,C,Sp
Ladder, fall protection	D,Co,F,Sp
Bolted connections	Co,Ps,C
Foundation, embedded section	D,Co,C
Foundation	D,C
Grounding/earthing strip	Cf,D,Co

453 **Acknowledgment**

454 This work was funded by SSE, SPR and the EPSRC (Grant No. EP/L016680/1).

455 **Bibliography**

- 456 [1] L. Ziegler, E. Gonzalez, T. Rubert, U. Smolka, and J. J. Melero,
 457 “Lifetime extension of onshore wind turbines: A review covering
 458 Germany, Spain, Denmark, and the UK,” *Renewable and Sustainable*
 459 *Energy Reviews*, vol. 82, pp. 1261–1271, 2 2018. [Online]. Available:
 460 <http://linkinghub.elsevier.com/retrieve/pii/S1364032117313503>
- 461 [2] DNV GL, “Service Specification: Certification of life-
 462 time extension of wind turbines,” 2016. [Online].
 463 Available: <https://rules.dnvgl.com/docs/pdf/DNVGL/SE/2016-03/DNVGL-SE-0263.pdf>
 464
- 465 [3] —, “Standard: Lifetime extension of wind turbines,” 2016. [On-
 466 line]. Available: <https://rules.dnvgl.com/docs/pdf/DNVGL/ST/2016-03/DNVGL-ST-0262.pdf>
 467
- 468 [4] T. Rubert, D. McMillan, and P. Niewczas, “A decision
 469 support tool to assist with lifetime extension of wind
 470 turbines,” *Renewable Energy*, 12 2018. [Online]. Available:
 471 <http://linkinghub.elsevier.com/retrieve/pii/S0960148117312685>

- 472 [5] —, “The Effect of Upscaling and Performance Degradation
473 on Onshore Wind Turbine Lifetime Extension Decision Mak-
474 ing,” *Journal of Physics: Conference Series*, vol. 926, p.
475 012013, 11 2017. [Online]. Available: [http://stacks.iop.org/1742-](http://stacks.iop.org/1742-6596/926/i=1/a=012013?key=crossref.63b19258ed5ed2069d531236b4256c69)
476 [6596/926/i=1/a=012013?key=crossref.63b19258ed5ed2069d531236b4256c69](http://stacks.iop.org/1742-6596/926/i=1/a=012013?key=crossref.63b19258ed5ed2069d531236b4256c69)
- 477 [6] K. Smarsly, D. Hartmann, and K. H. Law, “An Integrated Monitoring
478 System for Life-Cycle Management of Wind Turbines,” *International*
479 *Journal of Smart Structures and Systems*, vol. 12, no. 2, pp. 209–233,
480 2012.
- 481 [7] C. Rebelo, M. Veljkovic, L. S. Da Silva, R. Simes, and J. Henriques,
482 “Structural monitoring of a wind turbine steel tower - Part I: System
483 description and calibration,” *Wind and Structures, An International*
484 *Journal*, vol. 15, no. 4, pp. 285–299, 2012.
- 485 [8] C. Rebelo, M. Veljkovic, R. Matos, and L. Simes Da Silva, “Structural
486 monitoring of a wind turbine steel tower - Part II: Monitoring results,”
487 *Wind and Structures, An International Journal*, vol. 15, no. 4, pp. 301–
488 311, 2012.
- 489 [9] C. Loraux and E. Brühwiler, “The use of long term monitoring data
490 for the extension of the service duration of existing wind turbine
491 support structures,” *Journal of Physics: Conference Series*, vol. 753,
492 p. 072023, 9 2016. [Online]. Available: [http://stacks.iop.org/1742-](http://stacks.iop.org/1742-6596/753/i=7/a=072023?key=crossref.bb556abb5450ef12dd546de70c99ecb2)
493 [6596/753/i=7/a=072023?key=crossref.bb556abb5450ef12dd546de70c99ecb2](http://stacks.iop.org/1742-6596/753/i=7/a=072023?key=crossref.bb556abb5450ef12dd546de70c99ecb2)
- 494 [10] M. Botz, S. Oberlaender, M. Raith, and C. U. Grosse, “Monitoring of
495 Wind Turbine Structures with Concrete - steel Hybrid - tower Design,”
496 *8th European Workshop On Structural Health Monitoring (EWSHM*
497 *2016)*, no. August, pp. 5–8, 2015.
- 498 [11] M. Currie, F. Quail, and M. Saafi, “Development of a robust structural
499 health monitoring system for wind turbine foundations,” in *ASME turbo*
500 *expo 2012 Copenhagen*, 2012.
- 501 [12] M. Currie, M. Saafi, C. Tachtatzis, and F. Quail, “Structural
502 integrity monitoring of onshore wind turbine concrete foundations,”
503 *Renewable Energy*, vol. 83, pp. 1131–1138, 11 2015. [Online]. Available:
504 <http://linkinghub.elsevier.com/retrieve/pii/S0960148115003675>

- 505 [13] X. Bai, M. He, R. Ma, and D. Huang, “Structural condition
506 monitoring of wind turbine foundations,” *Proceedings of the Institution
507 of Civil Engineers - Energy*, pp. 1–19, 9 2016. [Online]. Available:
508 <http://www.icevirtuallibrary.com/doi/10.1680/jener.16.00012>
- 509 [14] M. Perry, J. McAlorum, G. Fusiek, P. Niewczas, I. McKeeman,
510 and T. Rubert, “Crack Monitoring of Operational Wind Turbine
511 Foundations,” *Sensors*, vol. 17, no. 8, p. 1925, 8 2017. [Online].
512 Available: <http://www.mdpi.com/1424-8220/17/8/1925>
- 513 [15] J. McAlorum, M. Perry, G. Fusiek, P. Niewczas,
514 I. McKeeman, and T. Rubert, “Deterioration of cracks
515 in onshore wind turbine foundations,” *Engineering Struc-
516 tures*, vol. 167, pp. 121–131, 7 2018. [Online]. Available:
517 <http://linkinghub.elsevier.com/retrieve/pii/S0141029617329644>
- 518 [16] T. Rubert, M. Perry, G. Fusiek, J. McAlorum, P. Niewczas,
519 A. Brotherston, and D. McCallum, “Field Demonstration of Real-Time
520 Wind Turbine Foundation Strain Monitoring,” *Sensors*, vol. 18, no. 2,
521 p. 97, 12 2017. [Online]. Available: [http://www.mdpi.com/1424-
522 8220/18/1/97](http://www.mdpi.com/1424-8220/18/1/97)
- 523 [17] N. Beganovic and D. Söffker, “Structural health management
524 utilization for lifetime prognosis and advanced control strategy
525 deployment of wind turbines: An overview and outlook concerning
526 actual methods, tools, and obtained results,” *Renewable and Sustainable
527 Energy Reviews*, vol. 64, pp. 68–83, 10 2016. [Online]. Available:
528 <http://linkinghub.elsevier.com/retrieve/pii/S1364032116301952>
- 529 [18] M. Luengo and A. Kolios, “Failure Mode Identification and
530 End of Life Scenarios of Offshore Wind Turbines: A Review,”
531 *Energies*, vol. 8, no. 8, pp. 8339–8354, 2015. [Online]. Available:
532 <http://www.mdpi.com/1996-1073/8/8/8339/>
- 533 [19] M. L. Wymore, J. E. Van Dam, H. Ceylan, and D. Qiao, “A survey of
534 health monitoring systems for wind turbines,” *Renewable and Sustain-
535 able Energy Reviews*, vol. 52, pp. 976–990, 12 2015. [Online]. Available:
536 <http://linkinghub.elsevier.com/retrieve/pii/S1364032115007571>

- 537 [20] T. Rubert, M. Perry, G. Fusiek, J. McAlorum, P. Niewczas,
538 A. Brotherston, and D. McCallum, “Field Demonstration of Real-Time
539 Wind Turbine Foundation Strain Monitoring,” *Sensors*, vol. 18, no. 1,
540 p. 97, 12 2017. [Online]. Available: <http://www.mdpi.com/1424-8220/18/1/97>
541
- 542 [21] H. J. Sutherland, *On the Fatigue Analysis of Wind Turbines*, Al-
543 buquerque, New Mexico, 1999.
- 544 [22] N. Stavridou, E. Efthymiou, and C. C. Baniotopoulos, “Welded con-
545 nections of wind turbine towers under fatigue loading: Finite element
546 analysis and comparative study,” *American Journal of Engineering and*
547 *Applied Sciences*, vol. 8, no. 4, pp. 489–503, 2015.
- 548 [23] European Union, “EN 1993-1-9 (2005): Eurocode
549 3: Design of steel structures - Part 1-9: Fa-
550 tigue,” 2005. [Online]. Available: [http://www.phd.eng.br/wp-
551 content/uploads/2015/12/en.1993.1.9.2005-1.pdf](http://www.phd.eng.br/wp-content/uploads/2015/12/en.1993.1.9.2005-1.pdf)
- 552 [24] ASTM, “Standard Practices for Cycle Counting in Fatigue Analysis.
553 Standard E1049-85,” 2011.
- 554 [25] F. Lueddecke, “Tower Flange Weld Assumption,” 2018.
- 555 [26] C. Loraux, “Long-term monitoring of existing wind turbine towers and
556 fatigue performance of UHPFCR under compressive stresses,” 2018.
557 [Online]. Available: <https://infoscience.epfl.ch/record/234540>
- 558 [27] IEC, “61400-13 2001,” pp. 0–4, 2003.
- 559 [28] European Union, “BS EN 1992-1-1:2004 - Eurocode 2: Design
560 of concrete structures - Part 1-1: General rules and rules
561 for buildings,” Tech. Rep., 2004. [Online]. Available: [ht-
562 tps://law.resource.org/pub/eu/eurocode/en.1992.1.1.2004.pdf](https://law.resource.org/pub/eu/eurocode/en.1992.1.1.2004.pdf)
- 563 [29] T. Burton, N. Jenkins, D. Sharpe, and E. Bossanyi, *Wind Energy*
564 *Handbook*. Chichester, UK: John Wiley and Sons, Ltd, 5 2011.
565 [Online]. Available: <http://doi.wiley.com/10.1002/9781119992714>
- 566 [30] C. Carrillo, A. Obando Montaña, J. Cidrás, and E. Díaz-Dorado,
567 “Review of power curve modelling for wind turbines,” *Renewable and*

- 568 *Sustainable Energy Reviews*, vol. 21, pp. 572–581, 5 2013. [Online]. Avail-
569 able: <http://linkinghub.elsevier.com/retrieve/pii/S1364032113000439>
- 570 [31] M. Lydia, S. S. Kumar, A. I. Selvakumar, and G. E.
571 Prem Kumar, “A comprehensive review on wind turbine power
572 curve modeling techniques,” *Renewable and Sustainable En-
573 ergy Reviews*, vol. 30, pp. 452–460, 2014. [Online]. Available:
574 <http://dx.doi.org/10.1016/j.rser.2013.10.030>
- 575 [32] M. I. Blanco, “The economics of wind energy,” *Re-
576 newable and Sustainable Energy Reviews*, vol. 13,
577 no. 6-7, pp. 1372–1382, 2009. [Online]. Available:
578 <http://linkinghub.elsevier.com/retrieve/pii/S1364032108001299>
- 579 [33] WindEurope, “Financing and investment trends,” 2016. [On-
580 line]. Available: [https://windeurope.org/about-wind/reports/financing-
581 investment-trends-2016/](https://windeurope.org/about-wind/reports/financing-investment-trends-2016/)
- 582 [34] J. Aldersey-Williams and T. Rubert, “Levelised cost of en-
583 ergy A theoretical justification and critical assessment,” *Energy
584 Policy*, vol. 124, pp. 169–179, jan 2019. [Online]. Available:
585 <https://linkinghub.elsevier.com/retrieve/pii/S0301421518306645>
- 586 [35] J. Olauson, P. Edström, and J. Rydén, “Wind turbine performance
587 decline in Sweden,” *Wind Energy*, 8 2017. [Online]. Available:
588 <http://doi.wiley.com/10.1002/we.2132>
- 589 [36] I. Staffell and R. Green, “How does wind farm performance decline
590 with age?” *Renewable Energy*, vol. 66, pp. 775–786, 2014. [Online].
591 Available: <http://dx.doi.org/10.1016/j.renene.2013.10.041>
- 592 [37] D. Vose, *Risk Analysis: A Quantitative Guide*. Wiley, 2008.
- 593 [38] D. J. Mundform, J. Schaffer, M.-J. Kim, D. Shaw, A. Thongteeraparp,
594 and P. Supawan, “Number of Replications Required in Monte Carlo
595 Simulation Studies: A Synthesis of Four Studies,” *Journal of Modern
596 Applied Statistical Methods*, vol. 10, no. 1, 8 2011. [Online]. Available:
597 <http://digitalcommons.wayne.edu/cgi/viewcontent.cgi?article=1285context=jmasm>
- 598 [39] S. J. Watson, P. Kritharas, and G. J. Hodgson, “Wind speed
599 variability across the UK between 1957 and 2011,” *Wind Energy*,

- 600 vol. 18, no. January 2015, pp. 21–42, 2013. [Online]. Available:
601 <http://onlinelibrary.wiley.com/doi/10.1002/we.1679/full>
- 602 [40] P. Tavner, D. M. Greenwood, M. W. G. Whittle, R. Gindele,
603 S. Faulstich, and B. Hahn, “Study of weather and location effects on
604 wind turbine failure rates,” *Wind Energy*, vol. 16, no. 2, pp. 175–187, 3
605 2013. [Online]. Available: <http://doi.wiley.com/10.1002/we.538>
- 606 [41] G. Wilson and D. McMillan, “Assessing Wind Farm Re-
607 liability Using Weather Dependent Failure Rates,” *Journal*
608 *of Physics: Conference Series*, vol. 524, p. 012181,
609 6 2014. [Online]. Available: [http://stacks.iop.org/1742-](http://stacks.iop.org/1742-6596/524/i=1/a=012181?key=crossref.b8dc65677e053e3646aa421e267e73ed)
610 [6596/524/i=1/a=012181?key=crossref.b8dc65677e053e3646aa421e267e73ed](http://stacks.iop.org/1742-6596/524/i=1/a=012181?key=crossref.b8dc65677e053e3646aa421e267e73ed)
- 611 [42] M. Reder and J. J. Meleró, “Modelling the effects of environmental
612 conditions on wind turbine failures,” *Wind Energy*, 5 2018. [Online].
613 Available: <http://doi.wiley.com/10.1002/we.2201>
- 614 [43] D. Cannon, D. Brayshaw, J. Methven, P. Coker, and D. Len-
615 aghan, “Using reanalysis data to quantify extreme wind power
616 generation statistics: A 33 year case study in Great Britain,”
617 *Renewable Energy*, vol. 75, pp. 767–778, 3 2015. [Online]. Available:
618 <http://linkinghub.elsevier.com/retrieve/pii/S096014811400651X>
- 619 [44] I. Tobin, R. Vautard, I. Balog, F.-M. Bréon, S. Jerez, P. M. Ruti,
620 F. Thais, M. Vrac, and P. Yiou, “Assessing climate change impacts
621 on European wind energy from ENSEMBLES high-resolution climate
622 projections,” *Climatic Change*, vol. 128, no. 1-2, pp. 99–112, 1 2015.
623 [Online]. Available: [http://link.springer.com/10.1007/s10584-014-1291-](http://link.springer.com/10.1007/s10584-014-1291-0)
624 [0](http://link.springer.com/10.1007/s10584-014-1291-0)
- 625 [45] Megavind, “Strategy for Extending the Useful Lifetime of a Wind Tur-
626 bine,” 2016.
- 627 [46] M. Schedat, T. Faber, and A. Sivanesan, “Structural health monitoring
628 concept to predict the remaining lifetime of the wind turbine structure,”
629 *Domestic Use of Energy, DUE 2016*, 2016.
- 630 [47] T. Q. Do, J. W. van de Lindt, and H. Mahmoud, “Fatigue Life Fragilities
631 and Performance-Based Design of Wind Turbine Tower Base Connec-

- 632 tions,” *Journal of Structural Engineering*, vol. 141, no. 7, p. 04014183,
633 2015.
- 634 [48] A. Mehmanparast, J. Taylor, F. Brennan, and I. Tavares, “Experimental
635 investigation of mechanical and fracture properties of offshore wind
636 monopile weldments: SLIC interlaboratory test results,” *Fatigue &
637 Fracture of Engineering Materials & Structures*, no. May, pp. 1–17, 5
638 2018. [Online]. Available: <http://doi.wiley.com/10.1111/ffe.12850>
- 639 [49] D. Helm, “Cost of Energy Review,” 2017.